Eur Biophys J (2007) 36:1019–1027
DOI 10.1007/s00249-007-0169-8

ORIGINAL PAPER

Variability in secondary structure of the antimicrobial peptide Cateslytin in powder, solution, DPC micelles and at the air–water interface

Frantz Jean-François · Lucie Khemtémourian · Benoît Odaert · Sabine Castano · Axelle Grélard · Claude Manigand · Katell Bathany · Marie-Hélène Metz-Boutigue · Erick J. Dufourc

Received: 15 February 2007 / Revised: 13 April 2007 / Accepted: 15 April 2007 / Published online: 7 July 2007

Abstract Cateslytin (bCGA ^{344}RSMRLSFRARGYGFR^{358}), a five positively charged 15 amino-acid residues arginine-rich antimicrobial peptide, was synthesized using a very efficient procedure leading to high yields and to a 99% purity as determined by HPLC and mass spectrometry. Circular dichroism, polarized attenuated total reflectance fourier transformed infrared, polarization modulation infrared reflection Absorption spectroscopies and proton two-dimensional NMR revealed the flexibility of such a peptide. Whereas being mostly disordered as a dry powder or in water solution, the peptide acquires a α-helical character in the "membrane mimicking" solvent trifuoroethanol. In zwitterionic micelles of dodecylphophatidylcholine the helical character is retained but to a lesser extent, the peptide returning mainly to its disordered state. A β-sheet contribution of almost 100% is detected at the air–water interface. Such conformational plasticity is discussed regarding the antimicrobial action of Cateslytin.

Keywords Antimicrobial peptides · Cateslytin · Circular dichroism · Solid phase synthesis · MALDI-TOF mass spectrometry · Solution NMR

Presented at the joint biannual meeting of the SFB-GEIMM-GRIP, Anglet France, 14–19 October, 2006.

F. Jean-François · L. Khemtémourian · B. Odaert · S. Castano · A. Grélard · C. Manigand · K. Bathany · E. J. Dufourc (✉)
UMR 5248 CBMN,
CNRS-Université Bordeaux 1-ENITAB, IECB,
2 rue Robert Escarpit, 33607 Pessac, France
e-mail: e.dufourc@iecb.u-bordeaux.fr

M.-H. Metz-Boutigue
INSERM Unité 575,
Physiopathologie du Système Nerveux,
Strasbourg, France

Present Address:
L. Khemtémourian
UMR 8601 LCBTP,
Université Renée Descartes,
75270 Paris Cedex 06, France

Introduction

The increasing resistance of bacteria to conventional antibiotics makes the development of new modes of treatment essential. Over the past few years, antimicrobial peptides were presented as a potential solution to this problem: whereas classical antibiotics act specifically on biosynthetic pathways, antimicrobial peptides may directly destabilize the lipid membrane (Shai 1999) and constitute a promising newly discovered strategy for the pharmaceutical industry. Most of the antimicrobial peptides are composed of L-amino acids, with defined α-helix or β-sheet secondary structures. Some are linear, mostly helical, without cysteines, while others contain one or more disulfide bonds, forming β-sheet or both β-sheet and α-helix structures (Shai 1999). In most cases, the peptide's mode of action appears to be by direct lysis of the pathogenic cell membrane (Dufourc et al. 1986, 1989; Oren and Shai 1998; Shai 1999). Despite extensive studies, the mode of action of this group of antibacterial and cytolytic polypeptides is not fully understood and the basis for their selectivity towards specific target cells is not known. Antimicrobial peptides resulting from the enzymatic degradation of Chromogranin A (CgA) and secreted during stress have been recently studied (Metz-Boutigue et al. 1998, 2003). The CgA is located in the secretary granules of most endocrine end neuroendocrine cells. Co-secreted

with several hormones and prohormones, the biological role of this 431 residues (49 kDa) acidic protein is not well known. The proteolysis of the CgA releases several peptides that seem to possess endocrine, paracrine, autocrine and neuro-immuno-modulatory properties. One of these, named Cateslytin ($bCgA_{344–358}$) (Taylor et al. 2000) was shown to possess new antimicrobial properties (Briolat et al. 2005). It was initially characterized for its inhibition of the catecholamine release from chromaffin cells (Mahata et al. 1997; Preece et al. 2004; Tsigelny et al. 1998). The synthesis and the purification of Cateslytin ($bCgA_{344–358}$) have already been reported (Briolat et al. 2005; Mahata et al. 1999, 2000) but incomplete information on the synthesis and the purification were given. No structural data is known on this peptide, but circular dichroism (CD) and Homology modeling have been performed on longer peptides. The CD performed on the extracted $bCgA_{344–364}$ showed substantial (63%) β-sheet structure in a hydrophobic environment (25% trifluoroethanol). The Homology modeling followed by molecular dynamics simulation on the bovine Catestatin ($bCgA_{342–370}$) in a water shell led to a β-strand/loop/β-strand structure (Tsigelny et al. 1998).

In order to further understand the antimicrobial mode of action of the Cateslytin ($bCgA_{344–358}$), we decided to optimize the complete protocol for synthesis and purification aiming at very high peptide purity. In a second part, structural investigations of this peptide were performed by CD, Polarized attenuated total reflectance Fourier transformed infrared (ATR-FTIR), Polarization modulation infrared reflection absorption spectroscopy (PMIRRAS) and NMR, as a dry powder or dissolved in various media such as water, trifluoroethanol (TFE) or dodecylphosphatidylcholine (DPC) micelles. This is the first step towards understanding the interaction between Cateslytin and membranes, which is currently under work in the laboratory.

Materials and methods

Chemicals

Fmoc-Arg (Pbf)-Novasyn TGA and Fmoc-Arg (Pbf)-Wang resin, 2-(1H-benzotriazole-1-yl)-1,1,3,3-tetramethyl-uronium hexafluorophosphate (HBtU), *N*-hydroxybenzotriazole (HOBt) and *N*-α-Fmoc-amino acids were purchased from VWR-NovaBiochem (Läufelfingen, Switzerland). Amino acids were protected as follows: t-butyl (tBu) for serine and tyrosine, 2,2,4,6,7-pentamethyl-dihydrobenzofuran-5-sulfonyl (pbf) for arginines. Piperidine, dichloromethane (DCM), dimethylformamide (DMF), diisopropylethylamine (DIEA) and acetic acid anhydride were purchased from SDS (Peypin, France); trifluoroacetic acid (TFA) was obtained from Applied Biosystems (Courtaboeuf, France); *N*-methylpyrrolidone (NMP) and triisopropylsilane (TIS) from ACROS organics (Geel, Belgium) and 1,2-ethanedithiol (EDT) from Aldrich (Saint Quentin Fallavier, France); acetonitrile for HPLC was of Grade A and obtained from Fischer (Geel, Belgium). Ultra high quality water (referred to as UHQ grade) was obtained through an Elga (Le Plessis Robinson, France) purification system. Deuterated dodecylphosphocholine-(DPC-$^2H_{38}$) and D_2O containing trimethylsilylpropionate (TMSP) were purchased from Euriso-Top (Gif-sur-Yvette, France). Dodecylphosphocholine (DPC) was purchased from Avanti Polar Lipids (Alabaster, USA).

Peptide synthesis

The syntheses were performed on an Applied Biosystems 433A Peptide Synthesizer (PE Biosystem, Courtaboeuf, France) using Fmoc strategy (Khemtémourian et al. 2005, 2006). The resins were preloaded with a protected arginine substituted at 0.21 mmol g^{-1} for the Novasyn TGA resin and 0.35 mmol g^{-1} for the Wang resin. Fastmoc chemistry was carried out in four major steps per cycle: (1) deprotection of Fmoc groups by piperidine, (2) activation of added amino acid with HBTU/HOBt (37.9/13.6 g) in 200 ml of DMF, (3) coupling by amide link formation with a solution of 35% DIEA in NMP and (4) capping to prevent truncated peptide elongation with acetic anhydride/DIEA/HOBt (19 ml/9 ml/0,8 g) in 400 ml of NMP. Each deprotection step was monitored by conductivity.

Cleavage from the resin

The cleavage solutions were prepared at 0°C and typically 10 ml was mixed with 0.4 g of peptide-containing resin. The final peptide mixture was cleaved from the resin and deprotected in 94% TFA including the following scavengers: 2.5% EDT, 2.5% water (UHQ), 1% TIS. Total deprotection and cleavage were achieved after 180 min in a covered Erlenmeyer. The peptide solution was then filtered under vacuum. The crude peptide was precipitated by adding 100 ml of cold diethyl ether and the cloudy aqueous phase was collected by filtration. The peptide was then dissolved in a mixture of water/acetonitrile (80/20) with 0.1% TFA, and lyophilized.

Purification and analysis

Two eluents have been used: water (UHQ) with 0.1% TFA (A) and acetonitrile with 0.08%TFA (B). Absorption was monitored at 214 nm. The crude peptide was dissolved at a 4-mg/ml concentration in an A/B ratio of (80/20; v/v) and purified by reverse-phase HPLC (Waters Alliance 2695,

Milford, MA, USA) using a A–B gradient. A semi-preparative Waters (Symmetry) C18 column (300 Å, 5 μm, 300 × 7.8 mm) was equilibrated in 80% of A at flow rate of 3 ml/min. Crude peptide solution measuring 250 μl (1 mg) of was loaded into a 2-ml loop, injected immediately onto the column at room temperature and eluted for over 16 min going from 20 to 22% of solvent B. All peptides were collected using ~80% of A.

MALDI-TOF mass spectrometry

Matrix-assisted laser desorption and ionization time of flight (MALDI-TOF) mass spectrometry (Vestal et al. 1995) was performed on a Bruker REFLEX III (Wissembourg, France) in the reflectron mode with a 20-kV acceleration voltage and a 23-kV reflector voltage. α-cyano-4-hydroxy-cinnamic acid (Sigma) was used as a matrix, prepared as a saturated solution of 50% acetonitrile/0.1% TFA in water. Peptide was mixed in a ratio 1:1 (v/v) with the matrix solution. Samples were prepared with the dried droplet method on a stainless steel target with 26 spots. External mass calibration was achieved with a mixture of eight peptides having masses ranging from 961 Da (fragment 4–10 of adrenocorticotropic hormone) to 3,495 Da (β-chain of oxidized bovine insulin).

Sample preparation for structural studies

CD measurements in aqueous solution were performed by dissolving the peptide in UHQ water, adjusted to pH = 7. Samples for micelles studies were prepared by hydrating the powder in UHQ water at DPC-to-peptide molar ratio of 100 (pH = 3.4). Cateslytin was dissolved in TFE at 8 mM for CD experiments and at 5 mM in a DPC-$^{2}H_{38}$ solution (UHQ water) at a DPC-to-peptide molar ratio of 100 (pH = 3) for NMR experiments. No peptide degradation was detected at this pH. A D_2O buffer (100 mM NaCl; 50 mM tris; adjusted to pH = 7.5 by dropwise addition of DCl) was used for ATR. The same buffer composition in H_2O was used for PMIRRAS experiments. Peptide concentration was measured by UV spectroscopy at 280 nm.

Circular dichroism

CD spectra were performed on a Mark VI Jobin dichrograph (Longjumeau, France), recorded at 0.5 nm intervals over the 180–270 nm wavelength range using a 0.1-mm pathlength quartz cell. The secondary structure studies were first achieved in water and TFE at room temperature for the following peptide concentrations: 50, 100, 250, 500, 1,000 μM. In DPC micelles the peptide concentration was 500 μM. Eight scans were performed. The experiments were run at 15-nm min^{-1}. To estimate the peptide secondary structure content, the relevant CD-spectra were converted into mean residue ellipticity [θ] (deg cm^2 $dmol^{-1}$) using the relationship $[\theta] = CD_{meas.}\,(degree)/(C(mol\ l^{-1}) \times l(cm) \times N_R \times 10)$, where N_R was the number of residues per peptide. Secondary-structure content was estimated from CD spectra using the deconvolution program CDFriend (S. Buchoux, unpublished). This program, developed in the laboratory, uses standard curves obtained for each canonical structure (α-helix, β-sheet, helix-II and random coil) with LiKj (alternated hydrophobic Leucine and hydrophilic/charged Lysine residues) peptides of known length, secondary structure (Castano et al. 1999, 2000) and CD spectrum. The program implements a simulated annealing algorithm to get the best combination of α-helix, β-sheet, helix-II and random coil that exhibits the lowest normalized root mean square deviation (NRMSD) with respect to the experimental spectrum. The procedure appeared to be robust, simple to use (no initial guesses) and well adapted for the secondary-structure characterization of amphiphilic peptides. The procedure will be described elsewhere. Accuracy is estimated to be ≤5%. Before deconvolution, experimental spectra were generally smoothed with a ten-point FFT Filter using the Origin Microcal software.

ATR spectroscopy

ATR spectra were recorded either on a Nicolet Magna 550 spectrometer equipped with a MCT detector cooled at 77 K or on a Nicolet Nexus 670 spectrometer equipped with a DTGS detector. The decomposition of the amide I and amide spectral region (1,580–1,700 cm^{-1}) into individual bands was performed with the Peaksolve (version 3.0, GRAMS) software and analyzed as a sum of Gaussian/Lorentzian curves, with consecutive optimization of amplitudes, band positions, half-width and Gaussian/Lorentzian composition of the individual bands.

Film formation and pressure measurement

Monolayer experiments were performed on a computer-controlled Langmuir film balance (Nima Technology, Coventry, England). The rectangular trough (V = 110 cm^3, S = 145 cm^2) and the barrier were made of Teflon. The surface pressure (Π) was measured by the Wilhelmy method using a filter paper plate. The trough was filled with the aqueous phosphate buffer using ultra pure water (Milli-Q, Millipore). The experiments were carried out at 25 ± 2°C. Pure Cateslytin films were obtained by deposition of few microliter of Cateslytin buffer stock solutions at the air/water interface to define the total peptide

concentration. Then, after ≈ 10 min the peptide film was slowly compressed up to 15 mN m^{-1}.

PMIRRAS spectroscopy

PMIRRAS spectra were recorded on a Nicolet Nexus 870 spectrometer equipped with a photovoltaic HgCdTe detector cooled at 77 K. Generally, 200 or 300 scans were coadded at a resolution of 4 cm^{-1}. In short, PMIRRAS combines FT-IR reflection spectroscopy with fast polarization modulation of the incident beam between parallel (Rp) and perpendicular (Rs) polarizations. Two-channel processing of the detected signal makes it possible to obtain the differential reflectivity spectrum:

$$\Delta R/R = (Rp - Rs) / (Rp + Rs)J2$$

To remove the contribution of liquid water absorption and the dependence on Bessel functions J2, the monolayer spectra are divided by that of the subphase. With an incidence angle of 75°, transition moments that preferentially orient in the plane of the interface give intense and upward-oriented bands whereas perpendicular ones give weaker and downward-oriented bands (Blaudez et al. 1994). The decomposition of the amide I and amide II spectral region (1,500–1,800 cm^{-1}) into individual bands was performed with the Peaksolve (version 3.0, Galactic) software and analyzed as a sum of Gaussian/Lorentzian curves, with consecutive optimization of amplitudes, band positions, half-width and Gaussian/Lorentzian composition of the individual bands.

NMR

Spectra were recorded on a Bruker Avance 500 WB Ultra Shielded NMR spectrometer using a 4 mm HR-MAS probe with z-gradient. The temperature in the rotor was 324 K (51°C) after correction for temperature increase due to air cushion friction at a magic angle spinning (MAS) speed of 5 kHz. Chemical shifts were referenced to the singlet (0.00 ppm) of trimethylsilylpropionate (TMSP). Phase-sensitive TOCSY (Total Correlation Spectroscopy) (Bax and Davis 1985a) and nuclear overhauser effect spectroscopy (NOESY) (Bax and Davis 1985b) were acquired using the states-TPPI mode. Sixty milliseconds spin lock time and 300 ms mixing time, respectively, were used. 4,096 (t2) × 512 (t1) data points and 128 scans per increment were used. For all experiments solvent suppression was performed using pre-saturation (Hore 1983) and Watergate (Piotto et al. 1992). Data processing and analysis was performed using the Topspin software.

Results

Synthesis and purification of Cateslytin

Two different synthesis pathways were tested with the aim of providing sufficient amounts of pure peptide. Both syntheses were carried out using the FastMoc strategy in a simple coupling mode, with 1 mmol of resin and fourfold excess of amino acids (medium range scale). The first synthesis was carried out with 416 mg of Novasyn TGA® resin that was preloaded with arginine. From 416 mg resin, 54 mg of crude peptide was obtained after cleavage (Fig. 1a). Analysis by MALDI-ToF (data not shown) led to a main peak at 1859.60 g mol^{-1}, in very good agreement

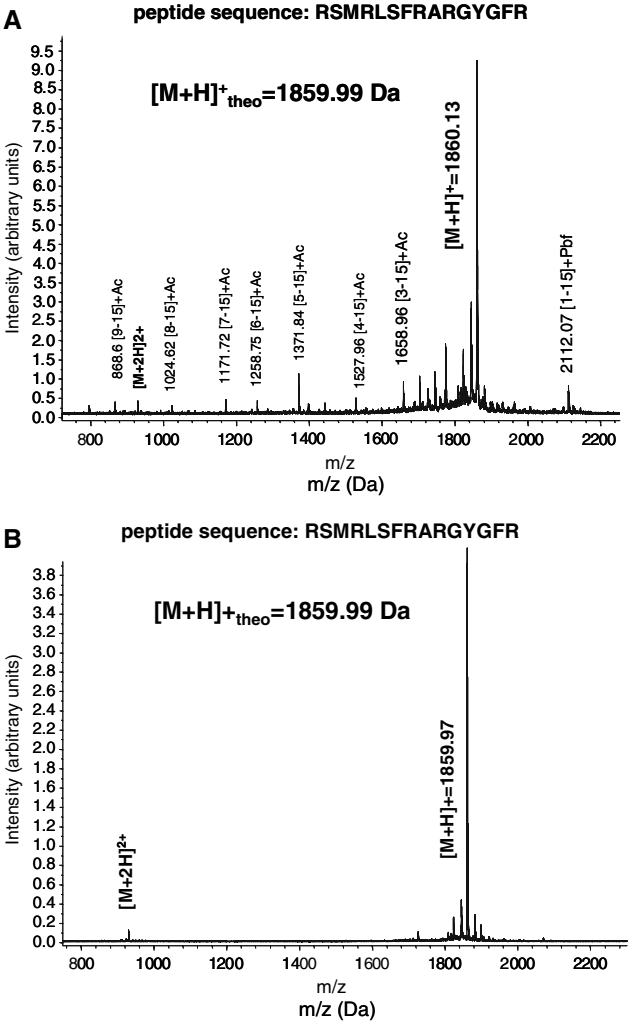

Fig. 1 MALDI-TOF spectrum of (**a**) the crude reaction mixture containing the 15 amino acid long Cateslytin fragments of the bovine CgA protein. The numbering in brackets [x-15] corresponds to truncated peptide segments. **b** Cateslytin after purification by reverse phase HPLC. The second ionization product is observed at $(M + nH)/(n)$, with a m/z of 930.36 Da. The lump before the main peak comes from degradation by the MALDI laser

with the theoretical molecular weight of 1859.99 g mol^{-1}. Purification on a semi-preparative C_{18} reverse-phase HPLC column was achieved as follows: after loading 3.5 mg of crude peptide, eluent B varied in a 10-min linear gradient from 10 to 28%, and then a 10-min linear gradient was applied from 28 to 34%. Cateslytin was eluted at a low percentage of acetonitrile (22%) after ca. 13 min. Peptide weighing 25 mg was recovered with a final purity of 84% as checked by MALDI-TOF and HPLC. The second synthesis was carried out with 286 mg of arginine-preloaded Wang resin. From 286 mg of resin, 143 mg of crude peptide were obtained after cleavage. The main peak of the mass spectrum indicates a molecular mass of 1859.60 g mol^{-1}, again in very good agreement with the theoretical molecular weight. The best purification was achieved on the same column with the following optimised conditions: 1 mg of crude mixture was loaded, then eluent B was varied in a 16 min linear gradient from 20 to 22% and Cateslytin was eluted 21% of acetonitrile with a retention time of ca. 13 min, Fig. 2. Fifty-seven milligrams of peptide were recovered; purity was checked by HPLC (Fig. 2b) using the Milenium software (Waters) and found to be 99%. MALDI-TOF (Fig. 1b) did not detect by-adducts.

Analysis by circular dichroism

Circular dichroism was used to assess the secondary structure of the synthetic peptide in aqueous solution, pH = 7, in TFE, pH = 6, and in DPC micelles, pH = 3. All experiments were performed at room temperature. Figure 3 shows the CD spectrum in water: a minimum is detected at 190 nm. In TFE a maximum is observed at 192 nm and two minima at 207 and 220 nm characteristic of α-Helices. In both aqueous and TFE solutions neither concentration-dependence nor temperature-dependence was noticed in CD measurements as indicated by no significant structural changes between 50 and 1,000 μM (data not shown) and between 15 and 45°C (data not shown), respectively. In DPC micelles three minima are detected at 185, 205 and 220 nm. Deconvolution of CD traces was performed, Table 1. In water and TFE the structure is mainly random (~90 and 60%, respectively). A weak percentage of *β*-sheet (~10%) is found in both media and a 30% α-helix is detected in the "membrane mimicking" solvent TFE. In DPC micelles the peptide is mostly random (76%) with a weak percentage of α-helix (6%) and 18% *β*-sheet.

Polarized ATR in powder and in solution

ATR experiments were performed at room temperature both on the dry powder and in hydrated conditions, Fig. 4.

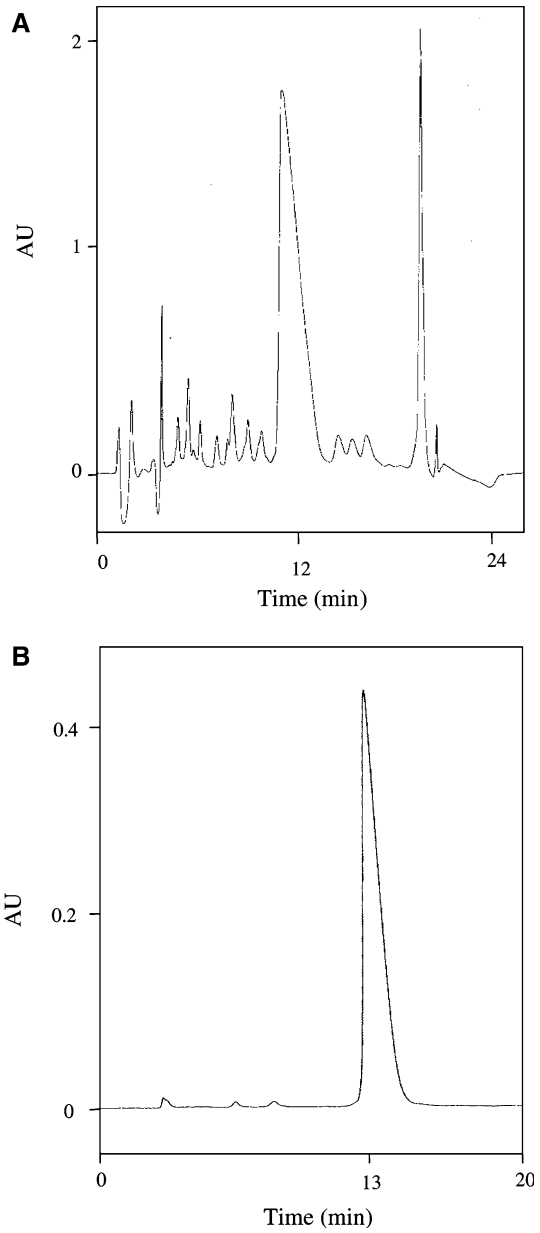

Fig. 2 Photodiode UV chromatograms at 214 nm of (**a**) the crude peptide after cleavage from the resin, (**b**) the purified peptide. Both used reverse-phase chromatography on a semi-preparative C18 column at a flow rate of 3 ml/min. The small peaks in (**a**) originate from truncated peptide segments. The major fraction was eluted after 13 min treatment with 21% of eluent B (see text)

Spectra display two bands in the amide I region: a main broad component around 1,650 cm^{-1} for the two systems characteristic of unstructured peptide, and a component around 1,625 cm^{-1} for the peptide powder and 1,615 cm^{-1} for the solution (and 1,685 cm^{-1}) characteristic of anti-parallel *β*-sheets (Barth and Zscherp 2002). There is also a third component in the water spectrum at 1,586 cm^{-1} due to the ionised form of arginine in D_2O. Decomposition of the amide I domain after baseline correction and subtraction

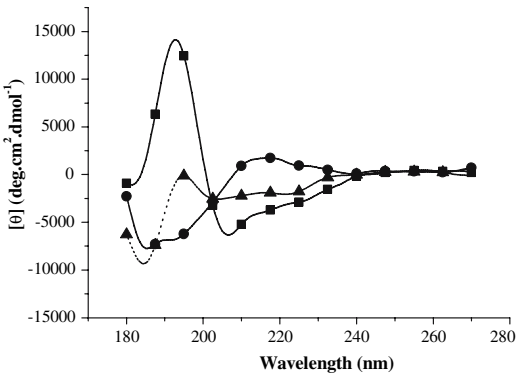

Fig. 3 Circular dichroism spectra of Cateslytin in water (*circles*), DPC micelles (*triangles*) and TFE (*squares*). The pH was 7 in pure water, 6 in pure TFE and 7.4 in buffer solution. Eight scans were accumulated at 25°C. Scan speed was set at 15 nm/min

Table 1 Secondary structure content of Cateslytin as a dry powder, dissolved in aqueous and TFE media and dispersed in aqueous DPC micelles

	α-Helix		β-sheet	∥ β-sheet	Anti-∥ β-sheet	β-turns	Random	
	CD	ATR	CD	ATR	ATR	ATR	CD	ATR
Dry powder	ND	0	ND	0	30	0	ND	70
Water	0	0	11	0	28	0	89	72
TFE	30	ND	10	ND	ND	ND	60	ND
DPC micelles	6	ND	18	ND	ND	ND	76	ND

Deconvolution of CD spectra was accomplished using the CD Friend deconvolution program (S. Buchoux, unpublished, see text). Accuracy is estimated to be of ca. 5%. Deconvolution of ATR spectra was accomplished using the Peaksolve (version 3.0, GRAMS) software deconvolution program. Accuracy is estimated to be of ca. 5%. All spectra were recorded at room temperature, ca. 20°C

ND = not determined

of the residual water band allows estimation of the secondary structure content, Table 1. Cateslytin is mainly unstructured (~70%) both in solution and powder. A ca. 30% of antiparallel β-sheet is nonetheless detected. A shift of the β-sheet band can also be noticed from 1,625 to 1,615 cm^{-1} when going from the dry powder to the hydrated system, which is characteristic of very strong hydrogen bond in β-sheet aggregates (Zandomeneghi et al. 2004).

PMIRRAS study of Cateslytin at the air–water interface

The in situ PMIRRAS spectra at the air–water interface of Cateslytin film during compression from 1 to 15 mN/m and decompression from 15 to 1 mN/m display well-resolved amide I bands between 1,600 and 1,700 cm^{-1} and a broad amide II band centered around 1,525 cm^{-1} (Fig. 5). The Amide I domain does not evolve during compression or

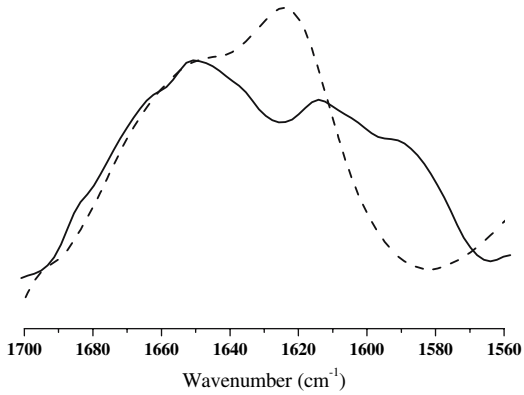

Fig. 4 ATR spectra of the amide I region of Cateslytin at room temperature. *Solid line*, water; *dashed line*, dry powder

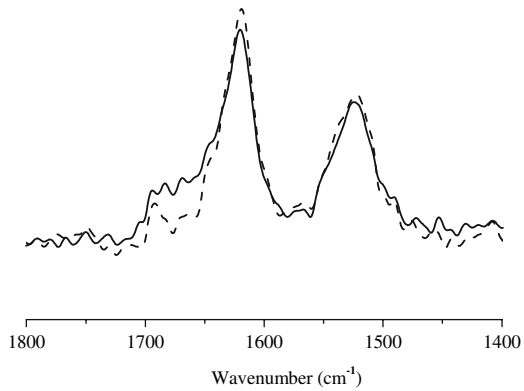

Fig. 5 PMIRRAS spectra of the amide I and II regions of Cateslytin at the air–water interface. *Solid line* 15 mM/m; *dashed line* 0.5 mN/m. Subphase: tris buffer (tris 50 mM, NaCl 100 mM, pH = 7.5, T = 23°C)

decompression and is centered around 1,620 and 1,694 cm^{-1}, which correspond to antiparallel β-sheets (Barth and Zscherp 2002). During all the compression/decompression process the strong amide I (1,620 cm^{-1})/amide I' (1,694 cm^{-1}) indicates that the β-sheets are mainly oriented flat on the interface plane (Castano et al. 1999, 2000; Cornut et al. 1996).

High resolution NMR in DPC micelles

The solution structure of the Cateslytin ($bCgA_{344\text{-}358}$) was investigated by homonuclear two-dimensional ^{1}H-NMR in DPC Micelles. An almost complete homonuclear chemical shift has been assigned (Table 2) from TOCSY and NOESY experiments. In Table 2 the chemical shifts values for Hα protons in a purely random structure as defined by Wishart et al. (1992) are also reported. For eight amino acids out of 13 the chemical shift values of α-protons are below the random range. Particularly the last six amino acids are well below this range, which is characteristic of α-helical character. Unfortunately, no {i, i + 3} correlation

Table 2 ^{1}H-NMR chemical shifts (ppm) of Cateslytin (bCgA344-358), at 324K, in DPC micelles, relative to TMSP (0 ppm)

	H^N	H^α		H^β	H^γ	Others
Arg_{344}			*4.38*			H^δ:- N^H:-
Ser_{345}			*4.50*			
Met_{346}	8.70	4.48	*4.52*	2.04	2.57	
Arg_{347}	8.33	4.29	*4.38*	1.81	1.60	H^δ:3.19 N^H:
Leu_{348}	8.08	4.34	*4.17*	1.60		H^δ:0.85/0.90
Ser_{349}	8.04	4.43	*4.50*	3.80		
Phe_{350}	8.15	4.22	*4.66*	3.05/3.15		**2,6**:7.22 **3,5**:7.27
Arg_{351}	8.11	4.24	*4.38*	1.78	1.55	H^δ:3.12 N^H:-
Ala_{352}	8.08	4.32	*4.35*	1.36		
Arg_{353}	8.05	4.23	*4.38*	1.84/1.76	1.6	H^δ:3.15 N^H:-
Gly_{354}	8.21	3.85	*3.97*			
Tyr_{355}	7.92	4.45	*4.60*	3.03/2.87		**2,6**:7.03 **3,5**:6.78
Gly_{356}	8.07	3.76–3.90	*3.97*			
Phe_{357}	7.97	4.24	*4.66*	3.16/3.00		**2,6**: 7.22 **3,5**:7.27
Arg_{358}	7.78	4.17	*4.38*	1.83/1.71	1.54	H^δ:3.12 N^H:-

Figures in italics are from the chemical shift index as defined by Wishart et al. (1992) and stand for random coil H^α values. H^N, H^α, H^β and H^γ are named according to IUPAC nomenclature

have been detected on the NOESY map, preventing determination of the 3D atomic structure.

Discussion

The major results of our study are twofold: (1) solid phase synthesis of Cateslytin is now well documented with a high yield and a very high purity, (2) its secondary structure is mainly random in powder, water and in DPC micelles, acquires helical character in TFE and is almost entirely in β-sheets oriented flat at the air–water interface. These different points will be discussed below.

Improved synthesis and purification of Cateslytin

In order to find optimal production conditions, we tested two different kinds of resins, three different cleavage pathways and several gradients. With the first synthesis (Novasyn resin) the synthesis yield is 37% and with the second synthesis (Wang resin), the synthesis yield is 88%. For a 15-residue peptide, the theoretical yield would be $0.99^{14} \times 100 = 87\%$, assuming 99% yield per step (Chan and White 2000; Fields et al. 1991). Not surprisingly, the Wang resin gives the maximum (theoretical) yield as already well documented for small and classical peptides such as ours. Our first cleavage trial was carried out with TFA/TIS/H_2O/EDT during 120 min. This mixture was not effective enough since we observed on the MS spectra one peak corresponding to the peptide with one pbf group indicating that the deprotection step is incomplete. The second and third trials were tested in parallel. For the second trial the same solution was used for 180 min and for the third a mixture of TFA/TIS/thioanisole/EDT/phenol crystalline was applied for 180 min. Both gave good results since no peak corresponding to the pbf group was observed in the MS spectra, suggesting that cleavage time is a crucial parameter. The purity has noticeably increased from one synthesis to the other (from 84 to 99%). This increase is due to an optimisation of the purification conditions. For the first synthesis, the gradient is divided into two slopes, thus the small peptides are eluted at the beginning of the run and at the end of the gradient the desired peptides are eluted. This purification gives a purity of 84% due to the presence of an undesired peptide that was eluted with Cateslytin. Even after two purifications, it was not possible to separate these two peptides. In the second synthesis the purification gradient chosen was almost isocratic. This purification allowed the separation of the undesired peptide that was eluted before the pure product.

Different structures in various media

CD and ATR spectroscopy of Cateslytin as dry powder or dissolved in water show that it is mainly unstructured (70–90% of random coil), which is not surprising for a small peptide. A small discrepancy is observed using both techniques in water. It is attributed to very different working concentrations and to the fact that ATR mainly gives information on interfaces depending on IR-beam penetration contrary to CD, which takes into account the entire volume of the cell. A small percentage of β-sheet is nonetheless detected both in powder and in water. Interestingly, an almost pure β-sheet is detected at the air–water interface, which is informative of what may predominate at the membrane interface. These analyses confirm the previous results of Tsigelny et al. (1998) who showed by hydrophobic moment plot that the region going from Ser^{345} to Gly^{356} had a cationic amphiphilic character (alternating cationic and hydrophobic residues) suggesting amphiphilic β-sheet. Moreover, the shift of the amide I band of the antiparallel β-sheet from 1,625 to 1,615 cm^{-1}, when hydrating the system, is characteristic of a strengthening of the hydrogen bond in β-sheet aggregates (Zandomeneghi et al. 2004). Interestingly, in pure TFE, CD experiments show that the peptide is partially structured in α helix (30%). Again, it is well known that TFE promotes the α-helix conformation by strengthening peptide H-bonds and may interrupt the hydrophobic interaction and then the ternary structure formation (Luo and Baldwin 1997). Structuration, as seen by NMR and CD, is less marked in DPC micelles since a lower α-helical character is obtained. The β-sheet contribution is nonetheless still present. This

suggests that binding to a zwitterionic highly curved interface is not really effective, the overall secondary structure being mostly as in water. Interestingly the β-sheet is well defined at the flat air–water interface. The capability for this peptide to change structures according to media is interesting as it may adapt to membranes of various natures and local topologies and promote different biological effects. Experiments on both zwitterionic and negatively charged lipid membranes are currently under way in our laboratory, which give further enlightenments about Cateslytin behaviour when facing lipid bilayers (work in preparation).

Conclusion

A robust procedure to synthesize Cateslytin has been optimized based on a Wang resin and mild cleavage conditions. Simple purification conditions on reverse-phase HPLC columns led to a very high peptide purity (99%). Preliminary structural studies reveal that like the majority of antimicrobial peptides, the Cateslytin is mainly unstructured in water and tends to adopt a weak α-helical structure or a marked β-sheet in media that are thought to approach the membrane environment. This structural variability demonstrates the pleiomorphic character of this antibiotic peptide.

Acknowledgments We thank gratefully Professor Jean-Marie Schmitter (UMR 5248 CBMN) for his advices on reverse HPLC and Sep Pak purification. The Conseil Régional d'Aquitaine is thanked for equipment funding.

References

Barth A, Zscherp C (2002) What vibrations tell us about proteins. Q Rev Biophys 35:369–430

Bax A, Davis DG (1985a) MLEV-17-based two-dimensional homonuclear magnetization transfer spectroscopy. J Magn Reson 65:355–360

Bax A, Davis DG (1985b) Practical aspects of two-dimensional transverse NOE spectroscopy. J Magn Reson 63:207–213

Blaudez D, Buffeteau T, Cornut JC, Desbat B, Escafre N, Pezolet M, Turlet JM (1994) Polarisation modulation IRFT spectroscopy at the air–water interface. Thin Solid Films 242:146–150

Briolat J, Wu SD, Mahata SK, Gonthier B, Bagnard D, Chasserot-Golaz S, Helle KB, Aunis D, Metz-Boutigue MH (2005) New antimicrobial activity for the catecholamine release-inhibitory peptide from chromogranin A. Cell Mol Life Sci 62:377–385

Castano S, Desbat B, Laguerre M, Dufourcq J (1999) Structure orientation and affinity for interface and lipids of ideally amphipathics lytics LiKi(i = 2j) peptides. Biochim Biophys Acta 1416:176–194

Castano S, Desbat B, Dufourcq J (2000) Ideally amphipathic β-sheeted peptides at interfaces: structure, orientation, affinities for lipids and hemolytics activities. Biochim Biophys Acta 1463:65–80

Chan WC, White PD (2000) Fmoc solid phase peptide synthesis. A practical approach. Oxford University Press, London, pp 9–40

Cornut I, Desbat B, Turlet JM, Dufourcq J (1996) In situ study by polarisation modulated Fourier transform infrared spectroscopy of the structure orientation of lipids and amphipaticpapetides at the air/water interface. Biophys J 70:305–312

Dufourc EJ, Faucon JF, Fourche G, Dufourcq J, Gulik-Krywicki T, Le Maire M (1986) Reversible disc-to-vesicle transition of melittin-DPPC complexes triggered by the phospholipid acyl chain melting. FEBS Lett 201:205–209

Dufourc EJ, Bonmatin JM, Dufourcq J (1989) Membrane structure and dynamics by ^{2}H-and ^{31}P-NMR. Effects of amphipatic toxins on phospholipid and biological membranes. Biochimie 71:117–123

Fields CG, Lloyd DH, MacDonald RL, Otteson KM, Noble RL (1991) HBTU activation for automated Fmoc solid-phase peptide synthesis. Pept Res 4:95–101

Hore PJ (1983) Solvent suppresion in fourier transform nuclear magnetic resonance. J Magn Reson 55:283–300

Khemtémourian L, Sani MA, Bathany K, Gröbner G, Dufourc EJ (2005) Synthesis and secondary structure in membranes of the Bcl-2 anti-apoptotic domain BH4. J Pept Sci 12:58–64

Khemtémourian L, Lavielle S, Bathany K, Schmitter JM, Dufourc EJ (2006) Revisited and large-scale synthesis and purification of the mutated and wild type neu/erbB-2 membrane-spanning segment. J Pept Sci 12:361–368

Luo P, Baldwin RL (1997) Mechanism of helix induction by trifluoroethanol: a framework for extrapolating the helix-forming properties of peptides from trifluoroethanol/water mixtures back to water. Biochemistry 36:8413–8421

Mahata SK, O'Connor DT, Mahata M, Yoo SH, Taupenot L, Wu H, Gill BM, Parmer RJ (1997) Novel autocrine feedback control of catecholamine release. A discrete chromogranin a fragment is a noncompetitive nicotinic cholinergic antagonist. J Clin Invest 100:1623–1633

Mahata SK, Mahata M, Parmer RJ, O'Connor DT (1999) Desensitization of catecholamine release. The novel catecholamine release-inhibitory peptide catestatin (chromogranin A344–364) acts at the receptor to prevent nicotinic cholinergic tolerance. J Biol Chem 274:2920–2928

Mahata SK, Mahata M, Wakade AR, O'Connor DT (2000) Primary structure and function of the catecholamine release inhibitory peptide catestatin (chromogranin A(344–364)): identification of amino acid residues crucial for activity. Mol Endocrinol 14:1525–1535

Metz-Boutigue MH, Goumon Y, Lugardon K, Strub JM, Aunis D (1998) Antibacterial peptides are present in chromaffin cell secretory granules. Cell Mol Neurobiol 18:249–266

Metz-Boutigue MH, Kieffer AE, Goumon Y, Aunis D (2003) Innate immunity: involvement of new neuropeptides. Trends Microbiol 11:585–592

Oren Z, Shai Y (1998) Mode of action of linear amphipatic a-helical antimicrobial peptides. Biopolymers 47:451–463

Piotto M, Saudek V, Sklenar V (1992) Gradient-tailored excitation for single-quantum NMR-spectroscopy of aqueous-solutions. J Biolmol NMR 2:661–665

Preece NE, Nguyen M, Mahata M, Mahata SK, Mahapatra NR, Tsigelny I, O'Connor DT (2004) Conformational preferences and activities of peptides from the catecholamine release-inhibitory (catestatin) region of chromogranin A. Regul Pept 118:75–87

Shai Y (1999) Mechanism of the binding, insertion and destabilization of phospholipid bilayer membranes by alpha-helical antimicrobial and cell non-selective membrane-lytic peptides. Biochim Biophys Acta 1462:55–70

Taylor CV, Taupenot L, Mahata SK, Mahata M, Wu H, Yasothornsrikul S, Toneff T, Caporale C, Jiang Q, Parmer RJ, Hook VY, O'Connor DT (2000) Formation of the catecholamine release-inhibitory peptide catestatin from chromogranin A. Determination of proteolytic cleavage sites in hormone storage granules. J Biol Chem 275:22905–22915

Tsigelny I, Mahata SK, Taupenot L, Preece NE, Mahata M, Khan I, Parmer RJ, O'Connor DT (1998) Mechanism of action of chromogranin A on catecholamine release: molecular modeling of the catestatin region reveals a beta-strand/loop/beta-strand structure secured by hydrophobic interactions and predictive of activity. Regul Pept 77:43–53

Vestal M, Juhasz P, Martin SA (1995) Delayed extraction matrix-assisted laser desorption time of flight mass spectrometry. Rapid Commun Mass Spectrom 9:1044–1050

Wishart DS, Sykes BD, Richards FM (1992) The chemical shift index: a fast and simple method for the assignment of protein secondary structure through NMR spectroscopy. Biochemistry 31:1647–1651

Zandomeneghi G, Krebs MRH, Mccamon MG, Fändrich M (2004) FTIR reveals structural differences between native beta-sheet proteins and amyloid fibrils Prot Sci 13:3314–3321